

## Liquid Crystals

# Multifunctional supramolecular dendrimers with an s-triazine ring as the central core. Liquid crystalline, fluorescence and photoconductive properties.

Madalina Bucos<sup>[a]</sup>, Teresa Sierra,<sup>[a]</sup> Attilio Golemme,<sup>\*,[c]</sup> Roberto Termine,<sup>[c]</sup> Joaquín Barberá,<sup>[a]</sup> Raquel Giménez,<sup>[a]</sup> José Luis Serrano,<sup>[b]</sup> Pilar Romero<sup>\*,[a]</sup> and Mercedes Marcos<sup>\*,[a.]</sup>

**Abstract:** Novel liquid crystal (LC) dendrimers have been synthesized by hydrogen bonding between an s-triazine as the central core and three peripheral dendrons derived from bis(hydroxymethyl)propionic acid. Symmetric acid dendrons bearing achiral promesogenic units have been synthesized to obtain 3:1 complexes with triazine that exhibit LC properties. Asymmetric dendrons that combine the achiral promesogenic unit and an active moiety derived from coumarin or pyrene structures have been synthesized in order to obtain dendrimers with photophysical and electrochemical properties. The formation of the complexes was confirmed by IR, and NMR data. The liquid crystalline properties have been investigated by differential scanning

calorimetry, polarizing optical microscopy and X-ray diffractometry. All complexes displayed mesogenic properties, which were smectic in the case of symmetric dendrons and their complexes and nematic in the case of asymmetric dendrons and their dendrimers. A supramolecular model for the lamellar mesophase, based mainly on X-ray diffraction studies, has been proposed. The electrochemical behaviour of dendritic complexes was investigated by cyclic voltammetry. The UV-Vis absorption and emission properties of the compounds and the photoconductive properties of the dendrons and dendrimers have also been investigated

## Introduction

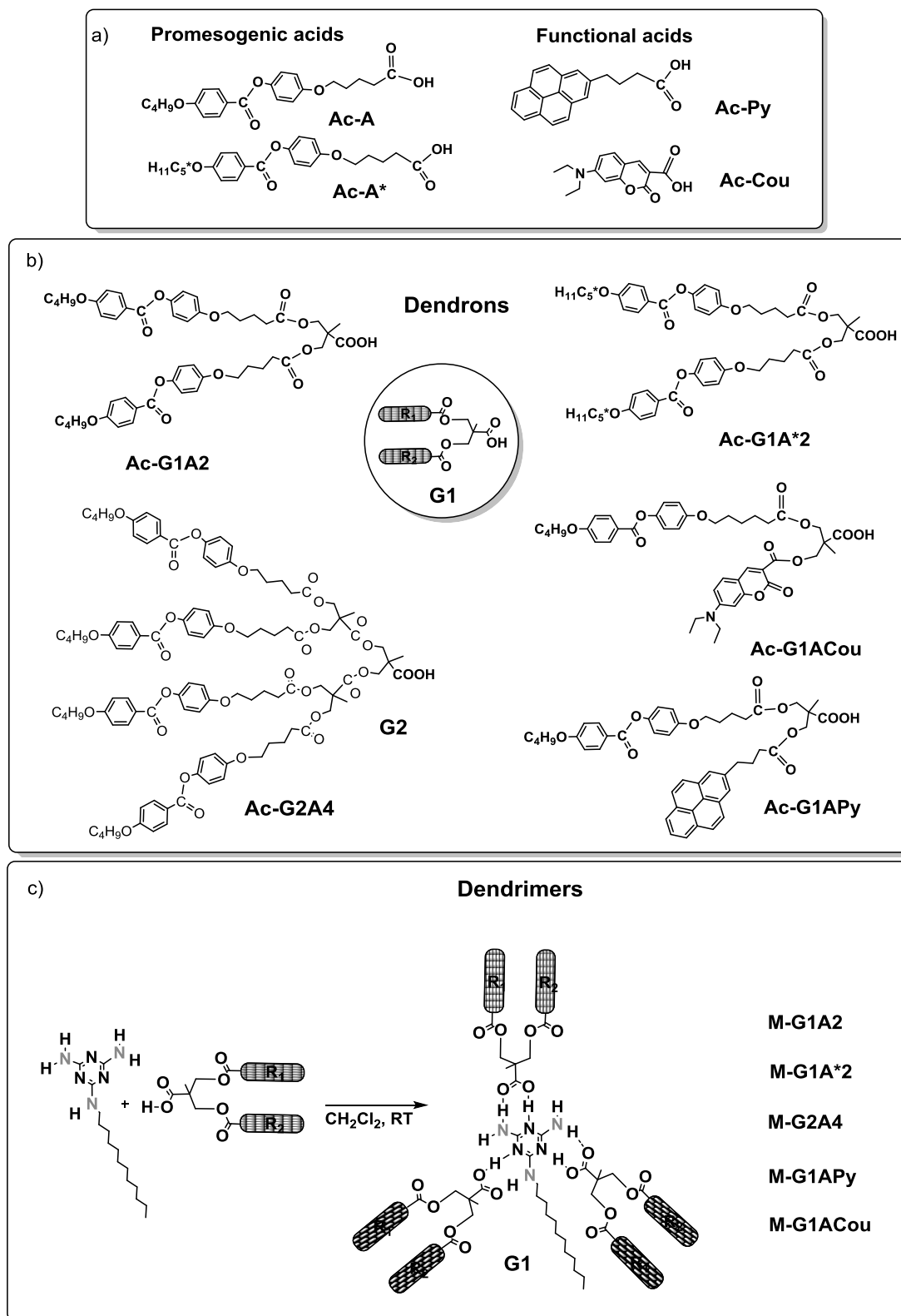
Dendrons and dendrimers are an important subclass within the dendritic polymer family.<sup>[1-4]</sup> The interest in these compounds is due to their special structural characteristics, which give them unique properties that differ from those of conventional polymers. These materials have a unique structure that grows from a focal

point with a defined number of radially attached branches as a function of the generation and peripheral functional groups. The increasing interest in these kinds of architectures arises from their applications in drug delivery, catalysis and advanced materials.<sup>[1-7]</sup> Dendrimers can be obtained by divergent or convergent iterative methods and many dendrimers have been built by the convergent union of dendrons. Although the preparation of dendrimers has improved over the past decade,<sup>[8]</sup> the larger and more complex structures still require major synthetic effort and this is often plagued by low yields and high polydispersity.<sup>[9]</sup> An alternative strategy is based on supramolecular chemistry, which allows the preparation of the dendrimers by a self-assembly process based on non-covalent interactions,<sup>[10]</sup> such as metal coordination chemistry,<sup>[11]</sup> hydrogen-bonding interactions<sup>[5]</sup> or electrostatic interactions.<sup>[12]</sup> In addition, dendrimers functionalized with promesogenic units can self-organize into liquid crystalline phases. Liquid crystal dendrimers present an attractive option to design functional materials that retain the inherent properties of dendrimers and provide well organized materials that are able to respond to external stimuli.<sup>[13]</sup>

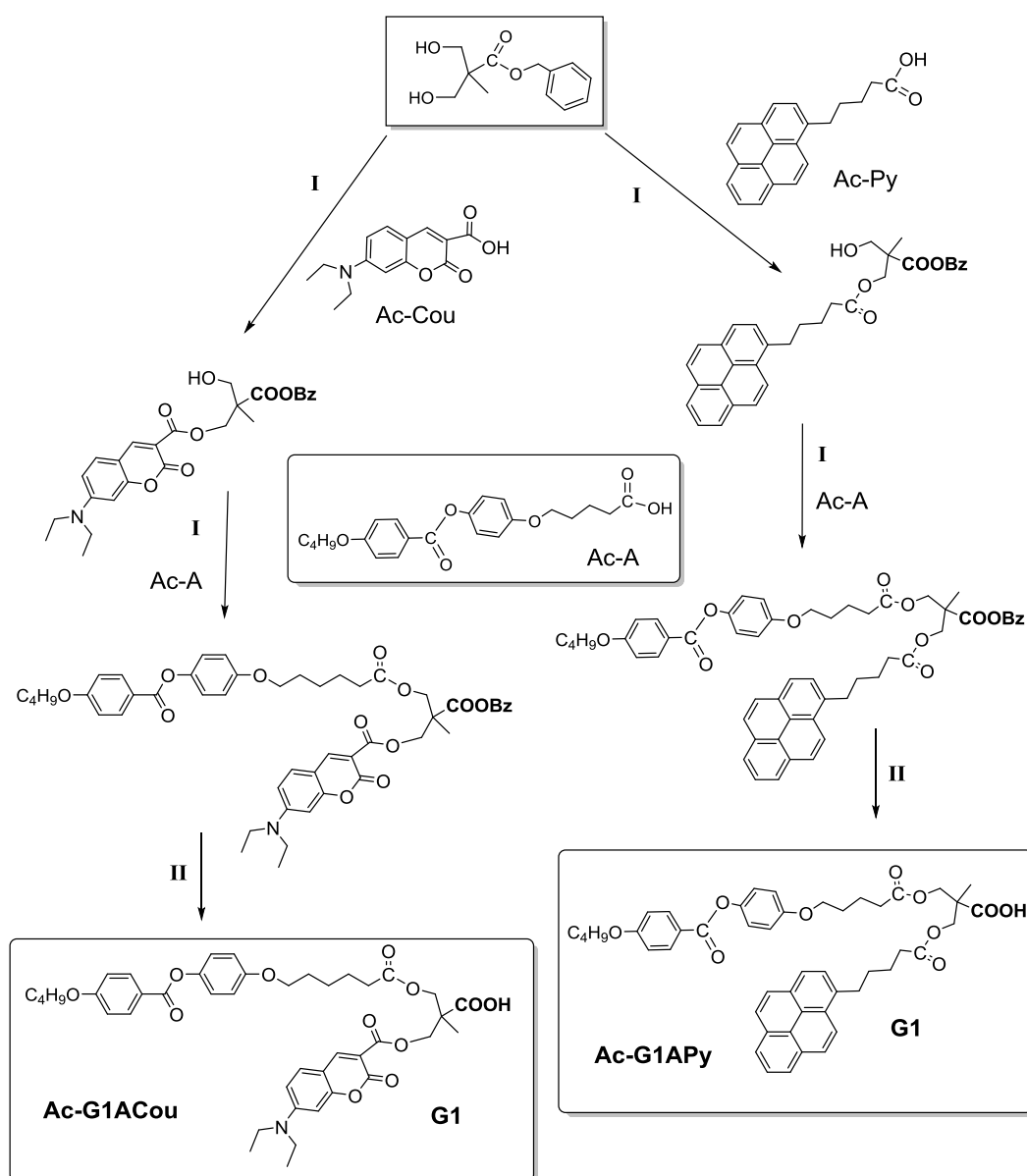
[a] M. Bucos, Dr. T. Sierra, Dr. J. Barberá, Dr. R. Giménez, Dr. P. Romero, Dr. M. Marcos.  
Departamento de Química Orgánica, Facultad de Ciencias-Instituto de Ciencia de Materiales de Aragón  
Universidad de Zaragoza-CSIC, 50009 Zaragoza (Spain).  
Tel: (+34) 976 762076  
E-mail: [promero@unizar.es](mailto:promero@unizar.es), [mmarcos@unizar.es](mailto:mmarcos@unizar.es)

[b] Prof. Dr. J. L. Serrano  
Departamento de Química Orgánica, Facultad de Ciencias-Instituto de Nanociencia de Aragón  
Universidad de Zaragoza-CSIC, 50009 Zaragoza (Spain).

[c] Dr. A. Golemme, Dr. R. Termine  
LASCAMM CR-INSTM, CNR-IPCF UOS CS-LiCryL, Dipartimento CTC. Università della Calabria, 87036 Rende (Italy).  
Tel: (+39) 098420 492016.  
E-mail: [a.golemme@unical.it](mailto:a.golemme@unical.it)



**Scheme 1.** Schematic representation of a) the promesogenic and functional units (**Ac-A**, **Ac-A\***, **Ac-Py** and **Ac-Cou**), carboxylic acid dendrons of the first and second generation and c) synthetic route to first generation of supramolecular dendrimers. Similarly, the synthesis of the second generation dendrimers was made starting from the dendron **Ac-G2A4**.



**Scheme 2.** Synthetic route for bifunctionalized carboxylic acid dendrons . (I) DCC, DPTS,  $\text{CH}_2\text{Cl}_2$ ; (II)  $\text{Pd}(\text{OH})_2/\text{C}$  20%, cyclohexene/THF

In 1998, Lehn and Zimmerman et al. reported the preparation of a dendrimer consisting of three H-bonded dendrons, which self-organized to give a thermotropic discotic liquid crystal.<sup>[14]</sup> Since then, a large number of supramolecular liquid crystal dendrimers obtained by the self-assembly of dendrons have been reported.<sup>[13e]</sup> Recently, we studied a new type of liquid crystal dendrimer functionalized with carbazole groups as hole-transporting moieties. These compounds were prepared by hydrogen bonding between a triazine core (**M**), as an electron-transporting unit, and three peripheral carboxylic acid dendrons derived from a bifunctionalized bis(hydroxymethyl)propionic acid (bis-MPA).<sup>[15]</sup> As a continuation of our research programme in this area, we present here four new families of liquid crystal dendrimers synthesized by hydrogen bonding between the

triazine central core (**M**) and three peripheral bifunctionalized dendrons derived from bis(hydroxymethyl)propionic acid (bis-MPA). The structures of the dendrons and dendrimers are shown in Scheme 1. Two types of symmetric bis-MPA-derived dendrons were synthesized: The first type is formed by the first and second generation dendrons functionalized with an achiral promesogenic unit (5-[4-(4-butoxybenzoyloxy)phenoxy]pentanoic acid) (**Ac-A**), the second one is formed by a first generation dendron containing a chiral promesogenic unit (5-[4-(4-((S)-2-methylbutoxy)benzoyloxy)phenoxy]pentanoic acid) (**Ac-A\***). Two types of bifunctionalized first generation dendrons bearing a unit of the achiral promesogenic unit **A** and a pyrene (**Py**: 1-pyrenebutyric acid) (**Ac-Py**) or coumarin (**Cou**: 7-(diethylamino)coumarin-3-carboxylic acid) (**Ac-Cou**) moiety were

also prepared in order to study their electrochemical and photophysical properties.

The triazine core (**M**) was selected in this work due to its ability to recognize other molecules by the donation and acceptance of hydrogen bonds, a characteristic that plays a key role in the self-organization of molecules and thus facilitates the formation of liquid crystals in low molecular weight compounds as well as in polymers or dendrimers.<sup>[16-17]</sup> Coumarin and pyrene were chosen to play the role of fluorophores in the dendrimer. Pyrene is a widely used probe due to its high fluorescence efficiency and excimer formation<sup>[18]</sup> and coumarin is biocompatible and highly valuable as a fluorescent chemosensor in a variety of fields.<sup>[19]</sup>

The aim of the work described here was to exploit mesomorphism as a tool to organize these functional dendrimers and to evaluate the luminescence and photoconductivity properties of these materials.

## Results and Discussion

### Synthesis of promesogenic units.

The achiral **Ac-A** and chiral **Ac-A\*** ester derivatives were prepared by previously reported procedures<sup>[15]</sup> (see SI, Scheme S3). The 1-pyrenebutyric acid was purchased from Sigma-Aldrich and it was used without further purification. 7-(Diethylamino)coumarin-3-carboxylic acid was prepared by the method described by Duan et al.<sup>[20]</sup> A short flexible spacer (1,4-butylene) was introduced in compounds **Ac-A**, **Ac-A\*** and **Ac-Py** in order to decorrelate the mesogenic units from the rest of the molecule and thus facilitate the molecular arrangement of these units within the mesophase.

### Synthesis of dendrons.

Carboxylic acid dendrons were prepared by DCC esterification between monomer 2,2-bis(hydroxymethyl)propionic acid (bis-MPA) protected by a benzyl ester group and the appropriate promesogenic acid. The benzyl ester group was subsequently removed efficiently by catalytic hydrogenolysis without affecting the ester bonds of the polyester backbone.<sup>[21]</sup> The synthetic routes followed to prepare the asymmetric and symmetric carboxylic acids are shown in Scheme 2 and Scheme S2, respectively.

### Typical procedure for the synthesis of the functionalized dendrimers.

The hydrogen-bonded complexes were prepared by mixing a CH<sub>2</sub>Cl<sub>2</sub> solution of the appropriate amount of each component (the triazine and the carboxylic acid dendron derivative in a 1:3 ratio) and slowly evaporating the solvent by stirring at room temperature. The general synthetic route for dendrimers is shown in Scheme 1.<sup>[16b]</sup>

Synthetic details and full characterization data for all promesogenic units, dendrons, dendrimers and their intermediates are provided in the Supporting Information.

### Structural characterization.

The structural characterization of the compounds was carried out by elemental analysis and spectroscopic methods: Fourier Transform Infrared spectroscopy (FTIR), Nuclear Magnetic Resonance (NMR) spectroscopy. The data are gathered in the SI. High-resolution mass of dendrons and their precursors by MALDI-TOF mass spectrometry are collected in Table S3 and Figures S1–S3.

The formation and stability of intermolecular H-bonding associations between the triazine and the dendrons were studied by infrared spectroscopy on neat samples as KBr pellets and by nuclear magnetic resonance (NMR) spectroscopy in deuterated solvents. The results confirmed the proposed structures of these materials.

### FT-IR Characterization.

The IR spectra of the complexes differed from those of the dendrons and triazine, especially in the regions corresponding to the carbonyl COOH and N–H groups, which are responsible for the interactions between molecules. As an example, (see SI, Figure S7, the stretching absorption at 1707 cm<sup>-1</sup> for carbonyl groups in dendron **Ac-G1ACou** is replaced by the shoulder at 1701 cm<sup>-1</sup> for complex **M-G1ACouA**. Significant modification of the bands corresponding to the free N–H groups of the triazine was also observed in the supramolecular dendrimer, and this proves that association takes place through the carboxylic acid group of the dendrons. Similar behaviour was observed for all the complexes (Figures S4–S8).

### NMR Characterization.

The chemical structures of the dendrons and the complexes were confirmed by one-dimensional <sup>1</sup>H and <sup>13</sup>C NMR spectroscopy and by two-dimensional <sup>1</sup>H-<sup>1</sup>H COSY, DOSY, <sup>1</sup>H-<sup>1</sup>H NOESY, <sup>1</sup>H-<sup>13</sup>C HSQC and <sup>1</sup>H-<sup>13</sup>C HMBC experiments. The <sup>1</sup>H and <sup>13</sup>C spectra of the dendrons and two-dimensional <sup>1</sup>H-<sup>1</sup>H NOESY spectrum for **M-G1A\*2**, <sup>1</sup>H-<sup>13</sup>C HSQC spectrum for **M-G1APy** and <sup>1</sup>H-<sup>13</sup>C HMBC spectrum for **Ac-G1ACou** are provided in the Supporting Information (see SI, Figures S9–S21).

The <sup>1</sup>H NMR spectra recorded on CDCl<sub>3</sub> solutions clearly show the formation of complexes, assuming that there is a rapid equilibrium between the complex and its components; the <sup>1</sup>H-NMR spectra of the triazine (**M**), bifunctionalized dendrons (**Ac-G1ACou** and **Ac-G1APy**) and complexes are shown in Figure S22 (see SI). All NH proton signals of the triazine derivative **M** are shifted downfield upon complexation as these protons are involved in the hydrogen bonds. The signals for the protons of the N-methylene group of the triazine alkyl chain are shifted to slightly higher field. In the dendron molecules, the acidic proton signals are very broad and are barely visible in the <sup>1</sup>H spectrum but they can be clearly observed in NOESY experiments due to molecular exchange with amino protons (see SI, Figure S19). The protons close to the H-bond experience slight displacements. For example, the methyl group signals move by around –0.03 ppm and the diastereotopic methylene (H<sub>s</sub>) signals by +0.04/+0.02 ppm. The change in the shape of these AB system signals after complexation is particularly noteworthy. The shift variations of the

signals of the main protons involved in complex formation are listed in Table S2.

DOSY and NOESY experiments were also employed to determine whether hydrogen bonding interactions are established between the triazine derivative **M** and the carboxylic acids. The self-diffusion of a chemical species in a solvent depends on its molecular size and hydrodynamic volume. According to this principle, the association of components leads to changes in the molecular diffusion coefficient and this can be used to detect the presence of a complex formed by hydrogen bonding in solution. Since there is fast exchange between the complex and the components on the NMR time scale, this value corresponds to the apparent diffusion coefficient of the complex and is a weighted average of the diffusion coefficients of both the bound and free components in the solvent. It is clear that these are the only coefficients measured for complexes and they are practically similar to those of the corresponding acids and much lower than those of the corresponding triazines (see SI, Figure S23).

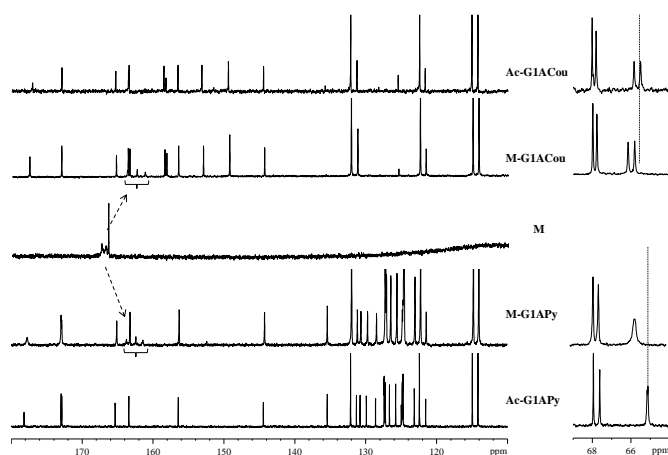


**Figure 1.** Expansions of  $^{13}\text{C}$  NMR spectra for complexes **M-G1ACou** and **M-G1APy** related to their dendrons or triazine (125 MHz,  $\text{CDCl}_3$ , 25 °C).

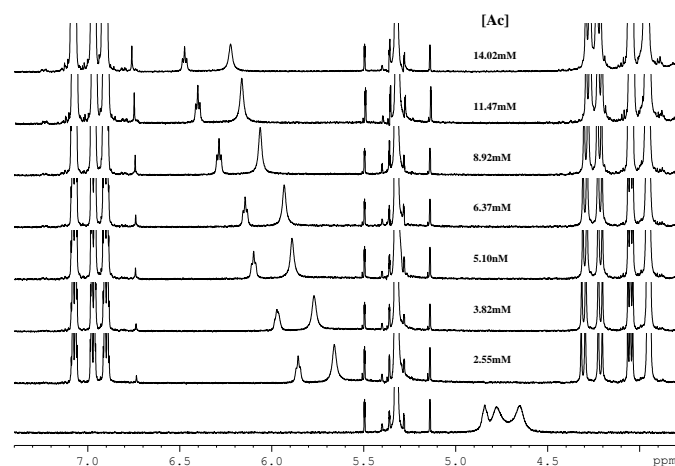


**Figure 2.**  $^1\text{H}$  NMR titration spectra of the complex **M-G1A2**. (500 MHz,  $[\text{D}_2]$ dichloromethane, 25 °C). The concentration of acid **Ac-G1A2** is increased while keeping the triazine concentration **[M]** constant at 2.55mM.

Variations in the chemical shifts of the  $^{13}\text{C}$  signals of carbon atoms involved in the formation of the supramolecular structure were also clearly observed. For example, the  $^{13}\text{C}$  signals of the triazine core are shifted to higher frequencies by 4 or 5 ppm and the  $^{13}\text{C}$  signals of the carboxylic acid groups and of the methylene groups in the  $\beta$ -position to the carboxylic acid group are shifted by +0.2–0.8 ppm after complexation (Figure 1).

We previously reported similar systems<sup>[22]</sup> and demonstrated that the stoichiometry of these complexes in solution is 1:1. Titration NMR experiments in  $[\text{D}_2]$ dichloromethane are shown in Figure 2 and allowed the estimation of the binding constant ( $718 \pm 98 \text{ M}^{-1}$  at 25 °C) for the complexation of the triazine derivative and the **Ac-G1A2** dendron. This value was calculated by nonlinear curve fitting of the chemical shifts.

The stoichiometry, however, was 3:1 in the bulk material when the molar amount of the acid was three times that of the triazine.<sup>[23]</sup>  $^{13}\text{C}$  CPMAS spectra of solid samples helped to confirm this stoichiometry (see SI, Figure S24).

### Thermal stability of the dendrimers and dendrons

The thermal stability of the dendrimers and dendrons was studied by thermogravimetric analysis (TGA) under a nitrogen atmosphere. All of the studied compounds exhibited good thermal stability and in all cases the 5% weight loss point is detected at temperatures more than 40 °C above the isotropization process. The dendrimer and dendrons of the second generation derived from **Ac-A** are slightly more stable than the homologous first generation compounds. Furthermore, the dendrons and dendrimers bearing the pyrene moiety are thermally more stable than the coumarin derivatives.

### Liquid Crystalline Properties

The mesomorphic behaviour of the compounds was analyzed by Polarized Optical Microscopy (POM), Differential Scanning Calorimetry (DSC) and X-ray diffraction (XRD). Three cycles were carried out in DSC experiments and data were taken from the second cycle. In some cases, the isotropization temperatures were taken from POM observations because transition peaks were not detected in DSC curves. The identification of the liquid crystal phase was carried out on the basis of POM observations and was confirmed by X-ray diffraction. The transition temperatures, mesophase type and the most relevant X-ray data for the dendrons and dendrimers synthesized are gathered in Table 1.

Only two precursor molecules exhibit liquid crystalline behaviour. The pure 2,4-diamino-6-dodecylamino-1,3,5-triazine (**M**) exhibits a monotropic smectic A mesophase (Cr 103 °C (SmA 39 °C) I).<sup>[16b]</sup> The 5-[4-(4-butoxybenzoyloxy)phenoxy]pentanoic acid (**Ac-A**) showed a nematic mesophase (C 91 N 104 I), identified by its *schlieren* texture and by the characteristic droplet optical texture observed when the nematic phase began to form

**Table 1. Mesomorphic behaviour, transition temperatures (°C) and X-ray diffraction results for dendrons and dendrimers under investigation. All of the diffractograms were recorded at room temperature**

Compound	Thermal data <sup>[a]</sup>	Mesophase X-ray study	Layer spacing d(Å) <sup>[c]</sup>	S per chain (Å <sup>2</sup> ) <sup>[d]</sup>
Ac-G1A2	g -3 SmC 75 SmA 81 I	SmC	- <sup>[e]</sup>	-
Ac-G2A4	g 10 SmC 91 N 94 I	SmC	38	40
Ac-G1A*2	g 4 SmC 25 C 82 I	SmC	- <sup>[e]</sup>	-
Ac-G1APy	g 14 N 90 I <sup>[b]</sup>	-	-	-
Ac-G1ACou	g 12 N 50 I <sup>[b]</sup>	-	-	-
M-G1A2	g 13 SmC 56 I	SmC	37.8	42.6
M-G2A4	g 9 SmC 85 I	SmC	38.5	41.8
M-G1A*2	g -1 SmC 20 I	SmC	39.4	42.0
M-G1APy	g 8 N 50 I <sup>[b]</sup>	-	-	-
M-G1ACou	g 14 N 60 I <sup>[b]</sup>	-	-	-

[a] Data obtained by DSC in the second heating process and taken at the maximum of the peak obtained at 10 °C/min. g: glass; C = crystal phase; N = nematic mesophase; SmC = smectic C mesophase; SmA = smectic A mesophase; I = isotropic liquid. [b] Optical data. [c] Smectic layer spacing. [d] Calculated cross-sectional area per chain (equivalent to the cross-sectional area per mesogenic unit) projected onto the smectic plane. [e] Crystallizes under the conditions of the X-ray diffraction experiment

on cooling the isotropic liquid. X-ray studies confirmed the nematic phase.

As can be seen from the results in Table 1, all of the dendrons and dendrimers synthesized behave as glassy materials at low temperatures (g transition in the range -3 to 14 °C) and all of them are liquid crystalline. Some representative examples of the DSC traces are shown in SI (Figures S25-S27). Dendron Ac-G1A\*2 exhibits semicrystalline behaviour, showing a glass transition below room temperature (Table 1). This behaviour has been previously described in dendrimers.<sup>[24]</sup> The DSC thermograms of the Ac-G2A4 dendron shows a crystal to mesophase transition in the first cycle, whereas, in the second and following scans only a glass transition appears.

Dendrons derived from acids **Ac-A** and **Ac-A\*** exhibit a smectic C phase at room temperature (see Figure 3). In addition, the dendrons **Ac-G1A2** and **Ac-G2A4**, show a smectic A or a nematic mesophase respectively, at higher temperatures and over a short temperature range. The corresponding supramolecular dendrimers exhibit, in all cases, a smectic C mesophase from room temperature. The mesophase was identified by optical microscopy (Figure S28), where a blurred schlieren texture and a broken fan-shaped texture were observed. On the other hand, the bifunctional dendrons and dendrimers bearing coumarin or pyrene moieties exhibit only nematic mesophases. The nematic nature of the phase was observed by optical microscopy on applying mechanical stress to the sample (Figure S28c, S28d) and was confirmed by X-ray diffraction. DSC scans show only a glass transition and the nematic to isotropic liquid transition temperature were determined by POM.

With the exception of the **M-G1ACou** complex, the mesophase temperature range is slightly smaller for the dendrimers than for the corresponding dendrons.

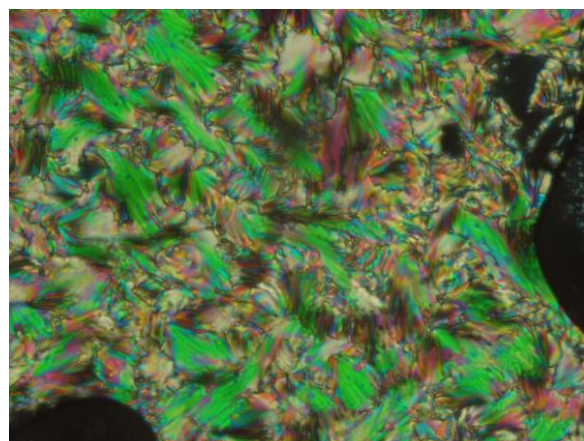


**Figure 3.** POM microphotograph of the smectic C mesophase of the dendron **Ac-G1A2** taken at 47 °C on cooling from the isotropic phase .

### Structural characterization of the mesophases

All of the compounds and complexes were investigated by X-ray diffraction with the aim of confirming the type of mesophase and determining the structural parameters. The mesophases were studied at room temperature and the data obtained are gathered in Table 1. In the case of dendrons **Ac-G1A2** and **Ac-G1A\*2** the X-ray study was not possible due to the tendency of these two compounds to crystallize under the conditions of the diffraction experiments. This tendency to crystallize is clearly illustrated for **Ac-G1A\*2** by the presence of an exothermic transition peak (cold crystallization) close room temperature detected by DSC in the heating process. In the case of **Ac-G1A2** crystallization was not observed by optical microscopy or by DSC; however, the sample crystallized after a few minutes when kept at room temperature during exposure to the X-rays. The tendency to crystallization persists at higher temperatures, which precluded the X-ray characterization of these two compounds under any set of conditions.

For all the remaining compounds and complexes, the X-ray patterns confirmed the nature of the mesophase assigned by optical microscopy (Table 1). Thus, the diffractograms of **Ac-G1APy**, **Ac-G1ACou** and their triazine complexes recorded in the nematic mesophase contain only diffuse scattered intensity, as expected given the absence of long-range positional order and the existence of long-range orientational order only (see SI, Figure S29) However, the orientational order is not reflected in the X-ray patterns due to the lack of macroscopic alignment in the bulk sample. The diffuse scattering arises from the short-range order of the fluctuating molecular positions in the nematic mesophase.

On the other hand, the smectic nature of the mesophases exhibited by **Ac-G2A4** and complexes **M-G1A2**, **M-G2A4** and **M-G1A\*2** was confirmed by the presence of one or two sharp reflections in the small-angle region in addition to a diffuse

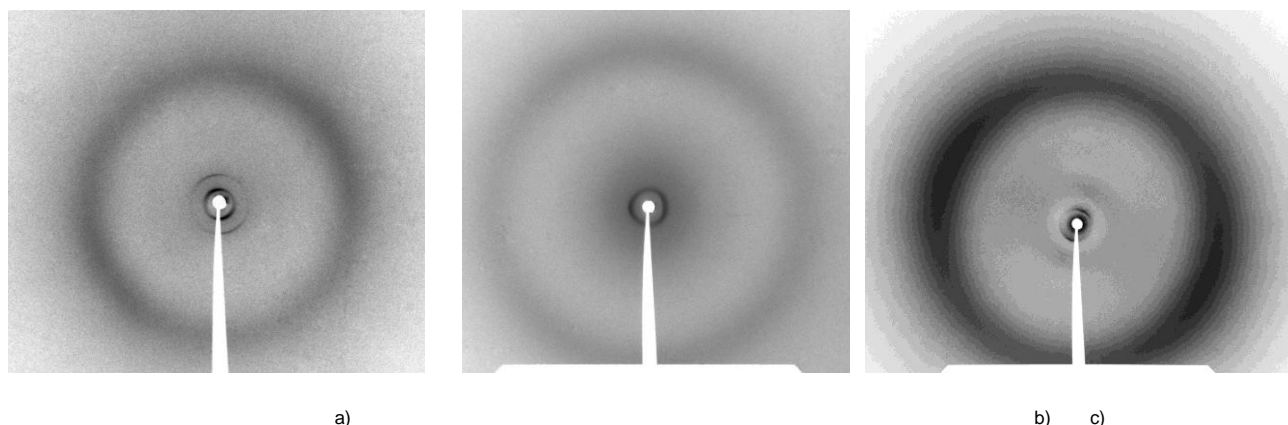


**Figure 4.** X-ray diffractograms of a) **M-G1A2**, b) **M-G1A\*2** and c) **M-G2A4** recorded in the smectic C phase at room temperature after cooling from the isotropic liquid

scattering band in the wide-angle region (Figure 4). When two small-angle maxima are detected, they are in the reciprocal spacing ratio 1:2. This confirms the lamellar organization and the two maxima are, respectively, the first and second order reflections from the periodically stacked layers. The large-angle halo arises from the interferences between the molten chains and other short-range intra- and intermolecular interferences in the direction perpendicular to the long axes of the molecules. Although this kind of pattern could correspond to either a smectic A or a smectic C organization, the room-temperature mesophases were assigned as smectic C on the basis of the optical textures (*vide supra*) and the structural parameters deduced from the X-ray measurements (*vide infra*). The experimentally measured layer spacing ( $d$  in Table 1) for **Ac-G2A4** is larger than the length of a single molecule in its most-extended conformation and shorter than twice its length. This is expected considering that the carboxylic acids are known to dimerize by H-bonding between the carboxyl group,<sup>[25]</sup> a process that generates the mesogenic entity.

The fact that the layer spacing is significantly shorter than twice the molecular length is due to a combination of two phenomena: (i) the conformational freedom of the chains as they are in a molten state in the mesophase, which reduces the effective molecule length; (ii) the tilt in the smectic mesophase.

The layer spacing for the complexes (Table 1) is similar to that measured for the dendron **Ac-G2A4**. In particular, this compound and its triazine complex have practically the same layer spacing. This is consistent with the fact that the triazine complex is a *trimer* of the dendron, in which the three molecules associated with the triazine core are statistically oriented in two opposite directions and are tilted with respect to the smectic layer (Figure 5). This arrangement must yield an overall molecular length very similar to that of the dimeric dendron. Thus, in the smectic mesophase the molecules of **Ac-G1A2** and **Ac-G1A\*2** and the molecules of **Ac-G2A4** contain, respectively, six or twelve mesogenic units statistically oriented in each direction.

This kind of molecular arrangement is similar to that previously found by some of us for other series' of covalent,<sup>[26]</sup>

ionic<sup>[27]</sup> and H-bonded<sup>[15]</sup> dendrimers that show smectic mesophases. The fact that the measured layer spacing is similar for the two dendron generations (compare  $d$  values for **M-G1A2** and **M-G2A4** in Table 1) supports our previous finding that, upon increasing the generation, the dendritic branches largely expand in the direction of the smectic plane. This produces a broadening of the molecule without a significant increase in length.

Additional support for this structural model and for the tilted nature of the mesophase of pure **Ac-G2A4** and of the three smectic complexes can be obtained from simple cross-section calculations. The molecular cross-sectional area  $A$  in  $\text{\AA}^2$  can be deduced as  $A = V / d$ , where  $V$  is the molecular volume in  $\text{\AA}^3$  and  $d$  is the experimentally measured layer spacing in  $\text{\AA}$ . For a density of  $1 \text{ g cm}^{-3}$ , which is typical for organic compounds, the molecular volume can be calculated using the following equation:  $V = M \times 10^{24} / N_A$

where  $M$  is the molar mass in g and  $N_A$  is Avogadro's number. On combining the two equations, the cross-sectional area of the molecule can be obtained as  $A = M \times 10^{24} / (d \times N_A)$ .

In the case of **Ac-G2A4** the cross-sectional area  $S$  per mesogenic unit (or per chain) can be obtained by dividing the total cross-section  $A$  by the number of mesogenic units oriented in each direction in the dimer, i.e. four. This gives a value of about  $40 \text{ \AA}^2$  (Table 1).

Similar values of  $S$  close to  $42 \text{ \AA}^2$  were obtained for the cross-sectional area per mesogenic unit in the case of the three smectic complexes. In this case, since each complex contains three molecules of the dendritic acid with their mesogenic units statistically oriented in each direction,  $S$  is obtained by dividing the total molecular cross-section by three for the first generation (**G1**) and by six for the second generation (**G2**). The hydrocarbon chain in the triazine does not affect these calculations because it is embedded in the central dendritic sublayer (Figure 5). The  $S$  values of  $40\text{--}42 \text{ \AA}^2$  obtained for both the acid and the complexes are too large for an orthogonal (smectic A) mesophase and are consistent with a tilted smectic mesophase, for which we can expect a larger value for the cross-sectional area of the mesogenic unit projected onto the smectic plane.<sup>[28]</sup> Moreover,

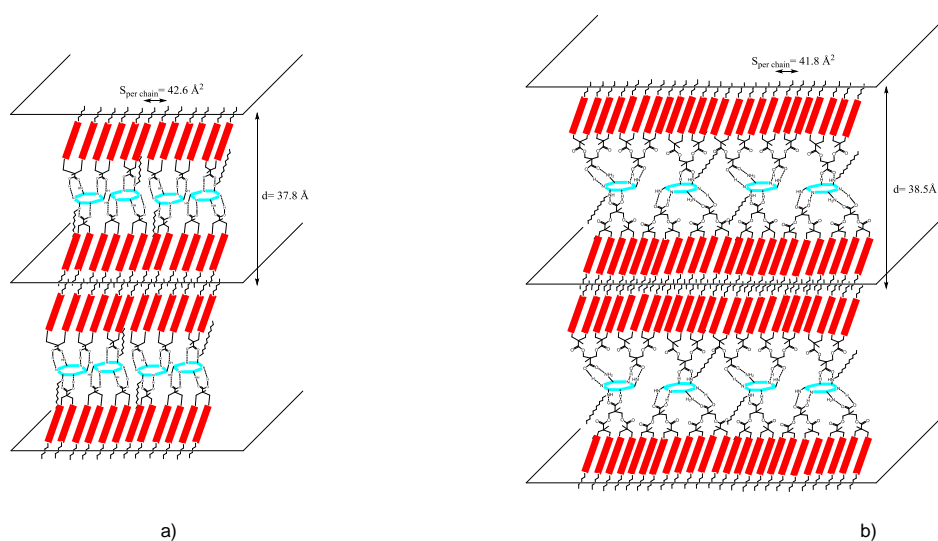


**Figure 5.** Proposed arrangement of the H-bonded complexes in the the smectic C mesophase of a) **M-G1A2** and b) **M-G2A4**. The blue rings represent the triazine cores and the red rectangles represent the mesogenic units.

the coherence between the  $S$  values obtained for all the compounds supports the aforementioned structural model proposed for the molecular conformation and layer packing in the mesophase, both for pure **Ac-G2A4** and the complexes

It is interesting to note that the large  $S$  values do not preclude the possibility that, in addition to tilting, there is some degree of interdigitation or partial intercalation between the terminal hydrocarbon chains of molecules in neighbouring layers. The tree-fold symmetry of the supramolecular dendrimers seems *a priori* to favour columnar mesomorphism, although the flexibility of the bis-MPA units allows the formation of a calamitic superstructure, as proposed in the models suggested by the X-ray studies, and only calamitic phases were observed.

The main difference between the symmetric and asymmetric derivatives is the type of mesophase that they exhibit, which is mainly lamellar for the former and nematic for the latter. Logically, the presence of two bulky groups such as the pyrene and coumarin units in the dendron and dendrimer derivatives introduces steric hindrance to the parallel molecular organization necessary to obtain the lamellar phase. Nevertheless, the intermolecular interactions of the neighbouring promesogenic units are strong enough to maintain the nematic order.

### Optical properties

The UV-Vis absorption and fluorescence spectra of the pyrene and coumarin dendrons **Ac-G1APy**, **Ac-G1ACou**, and **M-G1APy**, **M-G1ACou** dendrimers were measured in dilute dichloromethane

solution and in thin films (Figure 6). The data are collected in Table 2. Pyrene-containing dendrons and dendrimers show essentially the same spectra in dilute solutions and this is attributed to the characteristic absorption and emission bands of the pyrene chromophore in the monomeric form. However, the emission spectra of thin films show, in addition to the monomer emission, a broad emission band centered at 466–468 nm and this is due to excimer emission (Figure 6a).<sup>[29]</sup> In addition, in the absorption spectra of the thin films some line broadening and a slight red-shift is observed, which indicates some monomer preassociation. This indicates that the pyrene units must be spatially close to each other in order to exhibit the excimer emission band.

The coumarin dendron and dendrimers also display similar behaviour. In solution the absorption spectra show two bands at ca. 262 and 425 nm and these are typical of the coumarin chromophore.

The highest absorption band broadens and shows a blue-shift in the thin film spectra as a consequence of packing effects in the condensed phase. The emission spectra in solution display a band at 455–458 nm and this is related to the luminescence of the coumarin unit. However, in the thin film the emission is much broader and is considerably red-shifted at 530 nm (Figure 6b).

The results suggest that the coumarin units in the thin film of both dendron and dendrimer are aggregated, and this is consistent with results previously described for thin films of pure coumarin derivatives or for host materials doped at high concentrations.<sup>[19,30]</sup>



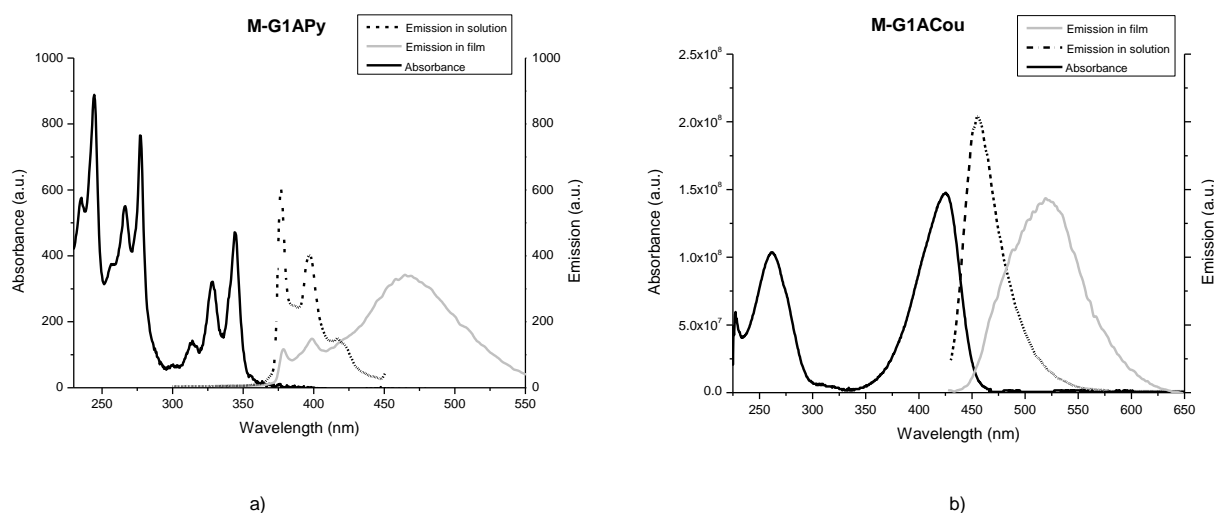


Figure 6. Absorption and fluorescence spectra in solution ( $\text{CH}_2\text{Cl}_2$ ), and fluorescence spectra in thin films for a) **M-G1APy** and b) **M-G1ACou**.

Table 2. Photophysical data for dendrons and dendrimers.				
Compound	$\lambda_{\text{abs}}$ (nm) ( $\text{CH}_2\text{Cl}_2$ )	$\lambda_{\text{abs}}$ (nm) (film)	$\lambda_{\text{em}}$ (nm) ( $\text{CH}_2\text{Cl}_2$ )	$\lambda_{\text{em}}$ (nm) (film)
<b>Ac-G1APy</b>	344	346	377	466
<b>M-G1APy</b>	344	348	377	468
<b>Ac-G1ACou</b>	425	416	458	531
<b>M-G1ACou</b>	425	417	455	530

Thus, the novel pyrene- and coumarin-containing dendrons and dendrimers exhibit quite different emission spectra in dilute solution and thin films. Thin films show emission characteristics typical of close packed pyrene or coumarin chromophores as spectra with dye-dye interactions are observed in all cases.

### Electrochemical properties

Cyclic voltammetry was performed on the pyrene and coumarin dendrons **Ac-G1APy**, **Ac-G1ACou** and their respective dendrimers **M-G1APy**, **M-G1ACou**, in order to calculate the energy level of the highest occupied molecular orbital (HOMO) of the dendrons and dendritic complexes containing the electroactive species pyrene and coumarin (Table 3). The measurements were performed in dichloromethane solutions under an argon atmosphere using a 3-electrode cell with a glassy carbon rod as the working electrode, Pt wire as the counter electrode and Ag/AgCl as the reference electrode. The potential was cycled between 0 and 2 V at a scan rate of  $100 \text{ mV s}^{-1}$  at  $25^\circ\text{C}$ . The solutions were  $10^{-4} \text{ M}$  in electroactive material and  $0.1 \text{ M}$  in tetrabutylammonium hexafluorophosphate as supporting

electrolyte. Ferrocene (Fc) was used as the internal reference ( $E_{1/2}(\text{Fc}/\text{Fc}^+) = 0.46 \text{ V}$ ) (Figure 7).

The dendron and dendrimer containing the pyrene unit showed similar behaviour, with two oxidation waves and the first oxidation potential at 1.35 V corresponding to the oxidation of the pyrene unit to its radical cation form (Figures 7a and 7b). For the coumarin-containing compounds three oxidation waves were observed in the case of the dendron and two waves for the dendrimer (Figures 7c and 7d). The first oxidation potential was found at lower values than for the pyrene compounds, at 1.27 V. In all cases the anodic peaks of all compounds are much more intense than the cathodic peaks. This marked asymmetry in the redox couple indicates that these species undergo irreversible oxidation.

Pyrene and coumarin compounds are all electron-donating and the coumarin derivatives are more easily oxidized. HOMO levels, which are related to the hole injection/transporting properties of the compounds, can be estimated from the first oxidation wave and the values are in the range expected for hole conductors.

Table 3. Cyclic voltammetry data for dendrons and dendrimers		
Compound	$E_{\text{ox}}$ (V)	HOMO (eV) <sup>[a]</sup>
<b>Ac-G1APy</b>	1.35	-5.69
<b>M-G1APy</b>	1.35	-5.69
<b>Ac-G1ACou</b>	1.27	-5.61
<b>M-G1ACou</b>	1.27	-5.61

[a]  $E_{\text{HOMO}} = -e [ E_{\text{ox}} - E_{1/2}(\text{Fc}/\text{Fc}^+) + 4.8 \text{ V} ]$ .

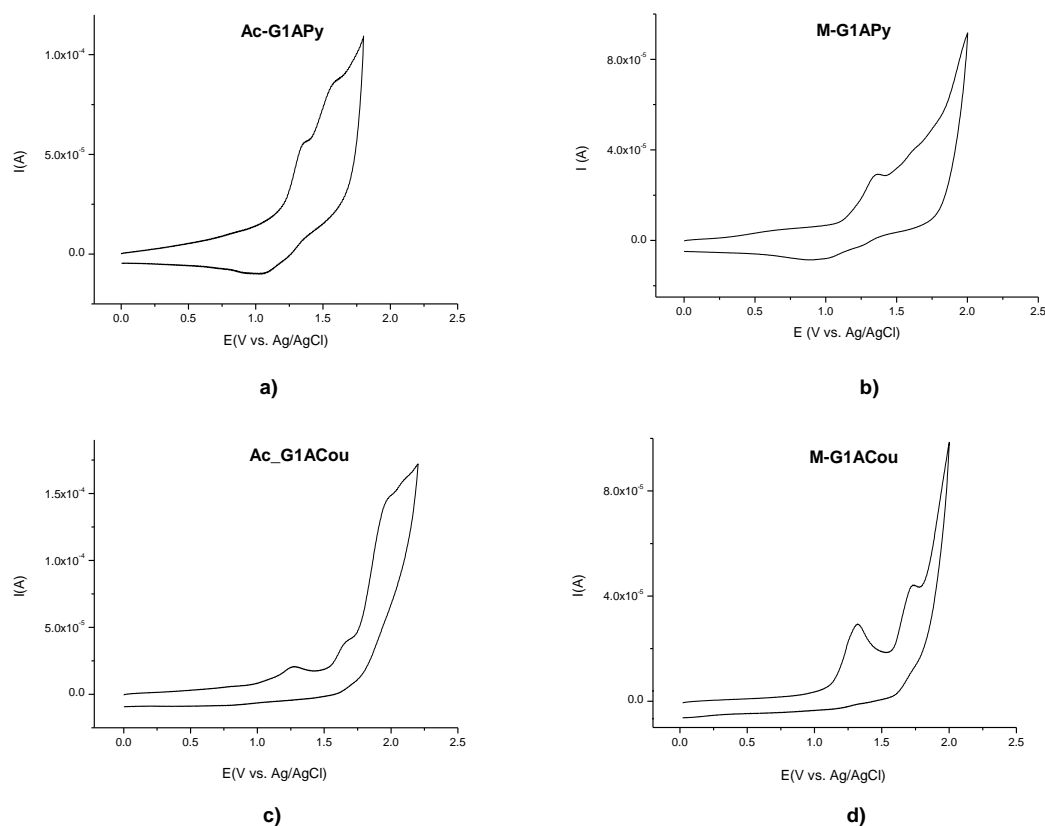


Figure 7. Voltammograms for (a) Ac-G1APy, (b) M-G1APy, (c) Ac-G1ACou, (d) M-G1ACou .

### Photoconductivity Studies

Photoconductivity measurements as a function of the applied electric field were performed on the two dendrons **Ac-G1APy** and **Ac-G1ACou** and on their respective dendrimers **M-G1APy** and **M-G1ACou**. Experimental details are included in the Supporting Information. Since photogeneration depends on the intensity  $I$  of the incident radiation, and the analyzed substances have a different light absorption coefficient  $\alpha$ , all of the experimental results are presented in terms of the normalized photoconductivity  $\sigma_{ph}/(I \alpha)$  in order to compare the results obtained for the different compounds. The observed photoconductivity as a function of the applied electric field is shown in Figure 8 for all four substances.

The curves for **M-G1APy** and **M-G1ACou** show a similar pattern of photoconductivity as a function of field. In particular, the photoconductivity does not vary significantly (it increases slightly) with the applied field. This behaviour can be attributed to the dependence of the charge mobility  $\mu$  on the applied field,<sup>[31]</sup> usually modelled as  $\ln \mu \propto E^{1/2}$ . The lack of a stronger field dependence for the photoconductivity, which is usually attributed to an increase in photogeneration quantum efficiency with higher fields,<sup>[32]</sup> could be taken as an indication that in the case of **M-G1APy** and **M-G1ACou** good levels of photogeneration can be achieved even at low fields. In turn, this might be attributed to the

simultaneous presence of an electron acceptor unit (the triazine) and a unit with a relatively strong donor character (coumarin or pyrene). Further studies will be necessary to confirm this hypothesis. Even if the dendrimers were not doped in order to

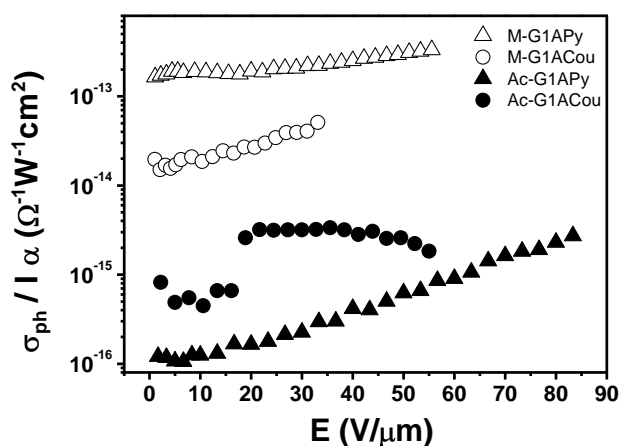


Figure 8. Normalized photoconductivity as a function of applied electric field for Ac-G1APy, Ac-G1ACou, M-G1APy and M-G1ACou. For the Ac-G1ACou data, the experimental error was much higher than in the other cases due to a much higher dark current.

increase photogeneration efficiency, their photoconduction is comparable to those measured in other non-crystalline organic photoconductors used as the active element in optoelectronic devices.<sup>[33]</sup>

The dendrons **Ac-G1APy** and **Ac-G1ACou** show a photoconductivity that is orders of magnitude lower than the photoconductivity of their respective dendrimers. Not surprisingly, it appears that the presence of a melamine core group, in addition to pyrene or coumarin, improves the photoconductivity, probably by improving the electron transport. Further conclusions cannot be drawn from the data in terms of the structure/property relation.

## Conclusion

We have designed and synthesized supramolecular liquid crystalline dendrimers with an *s*-triazine core and fluorescent dendrons incorporated in the periphery. The compounds were prepared using an easy and versatile method that involves H-bonding of dendritic carboxylic acids with 2,4-diamino-6-dodecyl-1,3,5-triazine.

All synthesized complexes displayed mesogenic properties; smectic in the case of monofunctionalized dendrons and their complexes and nematic in the case of bifunctionalized dendrons and dendrimers.

The novel pyrene- and coumarin-containing dendrons and dendrimers exhibit quite different emission spectra in dilute solution and in thin films. Thin films show emission characteristics typical of close packed pyrene or coumarin chromophores as spectra with dye-dye interactions are observed in all cases. HOMO levels, which are related to the hole injection/transporting properties of the compounds, can be estimated from the first oxidation wave, and they show values in the range of hole conductors. The dendrimers show a higher photoconductivity when compared to the dendrons, an effect that could be ascribed to two different factors, both a consequence of the presence of triazine. In fact, the triazine not only introduces a possible increase in electron mobility, but also may increase the efficiency of photogeneration due to the interaction between triazine and coumarin/pyrene. This latter effect is also suggested by the weak field dependence of the photoconductivity.

## Acknowledgments

This work was supported by the seventh FP THE PEOPLE PROGRAMME, The Marie Curie Actions; ITN, no. 215884-2, the MINECO, Spain, (under Projects: CTQ2012-35692 and MAT2012-38538-CO3-01), which included FEDER funding, and the Aragón Government-FSE (Project E04). AG and RT acknowledge support from the European Community's Seventh Framework Program (FP7 2007–2013) through the MATERIA Project (PONA3\_00370). Thanks are given to: Nuclear Magnetic Resonance, Mass Spectrometry, Elemental Analysis and Thermal Analysis Services of the CEQMA, Universidad de Zaragoza-CSIC (Spain). M. Bucos acknowledges support from the EU through an ESR fellowship

**Keywords:** Dendrimers • Hydrogen bonds • Liquid crystals • Fluorescence • Photoconductivity

[1] a) J. M. J. Fréchet, D. A. Tomalia, *Dendrimers and Other Dendritic Polymers*, John Wiley & Sons, Ltd, **2001**; b) D. A. Tomalia, J. B.

- Christensen, U. Boas, *Dendrimers, Dendrons, and Dendritic Polymers: Discovery, Applications, and the Future*, Cambridge University Press, **2012**.
- [2] G. R. Newkome, C. N. Moorefield, F. Vögtle, *Dendrimers and Dendrons: Concepts, Syntheses, Applications*, Wiley-VCH Verlag GmbH & Co. KGaA, **2001**.
- [3] F. Vögtle, G. Richardt, N. Werner, *Dendrimer Chemistry*, Wiley-VCH Verlag GmbH & Co. KGaA, **2009**.
- [4] D. Astruc, E. Boisselier, C. Ornelas, *Chem. Rev.* **2010**, *110*, 1857-1959.
- [5] a) F. W. Zeng, S. C. Zimmerman, *Chem. Rev.* **1997**, *97*, 1681-1712; b) S. C. Zimmerman, L. J. Lawless, *Dendrimers IV Book Series: Topics in Current Chemistry*, **2001**, Vol. 217, pp. 95-120.
- [6] A. M. Caminade, C. O. Turrin, R. Laurent, A. Ouali, B. Delavaux-Nicot, *Dendrimers: Towards Catalytic, Material and Biomedical Uses*, John Wiley & Sons, Ltd, **2011**.
- [7] a) D. A. Tomalia, *Chemistry Today* **2005**, *23*, 41-45; b) R. Hourani, A. Kakkar, *Macromol. Rapid Commun.* **2010**, *31*, 947-974; c) D. Astruc, *Nature Chemistry* **2012**, *4*, 255-267.
- [8] a) K. L. Killops, L. M. Campos, C. J. Hawker, *J. Am. Chem. Soc.* **2008**, *130*, 5062-5064; b) J. A. Johnson, M. G. Finn, J. T. Koberstein, N. J. Turro, *Macromol. Rapid Commun.* **2008**, *29*, 1052-1072; c) M. V. Walter, M. Malkoch, *Chem. Soc. Rev.* **2012**, *41*, 4593-4609.
- [9] a) D. A. Tomalia, A. M. Naylor, W. A. Goddard, *Angew. Chem. Int. Ed.* **1990**, *29*, 138-175; b) S. M. Grayson, J. M. J. Fréchet, *Chem. Rev.* **2001**, *101*, 3819-3867.
- [10] a) J. M. J. Fréchet, *Proc. Natl. Acad. Sci. U. S. A.* **2002**, *99*, 4782-4787; b) T. M. Hermans, M. A. C. Broeren, N. Gomopoulos, A. F. Smeijers, B. Mezari, E. N. M. Van Leeuwen, M. R. J. Vos, P. C. M. M. Magusin, P. A. J. Hilbers, M. H. P. Van Genderen, N. A. J. M. Sommerdijk, G. Fytas, Meijer, *J. Am. Chem. Soc.* **2007**, *129*, 15631-15638.
- [11] a) G. R. Newkome, R. Guther, C. N. Moorefield, F. Cardullo, L. Echegoyen, E. Perezcordero, H. Luftmann, *Angew. Chem. Int. Ed.* **1995**, *34*, 2023-2026; b) G. R. Newkome, E. F. He, C. N. Moorefield, *Chem. Rev.* **1999**, *99*, 1689-1746; c) H. J. Van Manen, F. C. J. M. Van Veggel, D. N. Reinhoudt, *Dendrimers IV Book Series: Topics in Current Chemistry*, **2001**, vol. 217, pp. 121-162; d) H.-B. Yang, A. M. Hawkrige, S. D. Huang, N. Das, S. D. Bunge, D. C. Muddiman, P. J. Stang, *J. Am. Chem. Soc.* **2007**, *129*, 2120-2129; e) B. Donnio, *Inorg. Chim. Acta* **2014**, *409*, Part A, 53-67.
- [12] a) M. Kawa, J. M. J. Fréchet, *Chem. Mater.* **1998**, *10*, 286-296; b) V. Chechik, M. Q. Zhao, R. M. Crooks, *J. Am. Chem. Soc.* **1999**, *121*, 4910-4911; c) A. G. Cook, U. Baumeister, C. Tschierske, *J. Mater. Chem.* **2005**, *15*, 1708-1721.
- [13] a) S. A. Ponomarenko, N. I. Boiko, V. P. Shibaev, *Polym. Sci., Ser. C* **2001**, *43*, 1-45; b) B. Donnio, D. Guillon, *Adv. Polym. Sci.* **2006**, *201*, 45-155; c) M. Marcos, R. Martin-Rapun, A. Omenat, J. L. Serrano, *Chem. Soc. Rev.* **2007**, *36*, 1889-1901; d) B. Donnio, S. Buathong, I. Bury, D. Guillon, *Chem. Soc. Rev.* **2007**, *36*, 1495-1513; e) B. M. Rosen, C. J. Wilson, D. A. Wilson, M. Peterca, M. R. Imam, V. Percec, *Chem. Rev.* **2009**, *109*, 6275-6540; f) C. Tschierske, *Angew. Chem. Int. Ed.* **2013**, *52*, 8828-8878; g) B. Dardel, R. Deschenaux, M. Even, E. Serrano, *Macromolecules* **1999**, *32*, 5193-5198; h) R. Deschenaux, B. Donnio, D. Guillon, *New J. Chem.* **2007**, *31*, 1064-1073; i) I. Bury, B. Heinrich, C. Bourgogne, G. H. Mehl, D. Guillon, B. Donnio, *New J. Chem.* **2012**, *36*, 452-468.
- [14] M. Suárez, J. M. Lehn, S. C. Zimmerman, A. Skoulios, B. Heinrich, *J. Am. Chem. Soc.* **1998**, *120*, 9526-9532.
- [15] S. Castelar, J. Barbera, M. Marcos, P. Romero, J.-L. Serrano, A. Golemme, R. Termine, *J. Mater. Chem. C* **2013**, *1*, 7321-7332.
- [16] a) S. Kumar, *Chemistry of Discotic Liquid Crystals: From Monomers to Polymers*, CRC Press/Taylor and Francis Group, **2011**; b) J. Barbera, L. Puig, P. Romero, J. L. Serrano, T. Sierra, *J. Am. Chem. Soc.* **2006**, *128*, 4487-4492; c) H. K. Dambal, C. V. Yelamaggad, *Tetrahedron Lett.* **2012**, *53*, 186-190; d) F. Yang, J. Xie, H. Guo, B. Xu, C. Li, *Liq. Cryst.* **2012**, *39*, 1368-1374; e) C. Domínguez, B. Heinrich, B. Donnio, S. Coco, P.

- Espinet, *Chem. Eur. J.* **2013**, *19*, 5988-5995; f) L.-L. Lai, S.-J. Hsu, H.-C. Hsu, S.-W. Wang, K.-L. Cheng, C.-J. Chen, T.-H. Wang, H.-F. Hsu, *Chem. Eur. J.* **2012**, *18*, 6542-6547; g) E. Beltran, J. Luis Serrano, T. Sierra, R. Gimenez, *J. Mater. Chem.* **2012**, *22*, 7797-7805.
- [17] a) D. Goldmann, R. Dietel, D. Janietz, C. Schmidt, J. H. Wendorff, *Liq. Cryst.* **1998**, *24*, 407-411; b) J. Barbera, L. Puig, P. Romero, J. L. Serrano, T. Sierra, *J. Am. Chem. Soc.* **2005**, *127*, 458-464; c) A. Kohlmeier, D. Janietz, S. Diele, *Chem. Mater.* **2006**, *18*, 1483-1489; d) S. Coco, C. Cordovilla, C. Dominguez, B. Donnio, P. Espinet, D. Guillon, *Chem. Mater.* **2009**, *21*, 3282-3289; e) A. Kohlmeier, L. Vogel, D. Janietz, *Soft Matter* **2013**, *9*, 9476-9486.
- [18] a) Y. Kamikawa, T. Kato, *Org. Lett.* **2006**, *8*, 2463-2466; b) Y. Sagara, T. Kato, *Angew. Chem. Int. Ed.* **2008**, *47*, 5175-5178.
- [19] S. R. Trenor, A. R. Shultz, B. J. Love, T. E. Long, *Chem. Rev.* **2004**, *104*, 3059-3078.
- [20] G. He, D. Guo, C. He, X. Zhang, X. Zhao, C. Duan, *Angew. Chem. Int. Ed.* **2009**, *48*, 6132-6135.
- [21] H. Ihre, A. Hult, J. M. J. Fréchet, I. Gitsov, *Macromolecules* **1998**, *31*, 4061-4068.
- [22] F. Vera, J. Barberá, P. Romero, J. L. Serrano, M. B. Ros, T. Sierra, *Angew. Chem. Int. Ed.* **2010**, *49*, 4910-4914.
- [23] F. Vera, R. M. Tejedor, P. Romero, J. Barbera, M. B. Ros, J. L. Serrano, T. Sierra, *Angew. Chem. Int. Ed.* **2007**, *46*, 1873-1877.
- [24] S. Hernandez-Ainsa, J. Barbera, M. Marcos, J. L. Serrano, *Soft Matter* **2011**, *7*, 2560-2568.
- [25] a) D. Demus, *Vol. 1* (Eds.: D. Demus, J. Goodby, G. W. Gray, H. W. Spiess, V. Vill), Wiley-VCH Verlag GmbH, **1998**, pp. 133-187; b) M. Qaddoura, K. Belfield, *Materials* **2010**, *3*, 827-840.
- [26] J. Barberá, M. Marcos, J. L. Serrano, *Chem. Eur. J.* **1999**, *5*, 1834-1840.
- [27] R. Martin-Rapun, M. Marcos, A. Omenat, J. Barbera, P. Romero, J. L. Serrano, *J. Am. Chem. Soc.* **2005**, *127*, 7397-7403.
- [28] J. Lenoble, S. Campidelli, N. Maringa, B. Donnio, D. Guillon, N. Yevlampieva, R. Deschenaux, *J. Am. Chem. Soc.* **2007**, *129*, 9941-9952.
- [29] F. M. Winnik, *Chem. Rev.* **1993**, *93*, 587-614.
- [30] T. Yu, P. Zhang, Y. Zhao, H. Zhang, J. Meng, D. Fan, *Org. Electron.* **2009**, *10*, 653-660.
- [31] H. Bässler, *Phys. Stat. Sol. B* **1993**, *175*, 15-56.
- [32] L. Onsager, *J. Che. Phys.* **1934**, *2*, 599-615.
- [33] a) E. Hendrickx, Y. Zhang, K. B. Ferrio, J. A. Herlocker, J. Anderson, N. R. Armstrong, E. A. Mash, A. P. Persoons, N. Peyghambarian, B. Kippelen, *J. Mater. Chem.* **1999**, *9*, 2251-2258; b) H. Li, R. Termine, N. Godbert, L. Angiolini, L. Giorgini, A. Golemme, *Org. Electron.* **2011**, *12*, 1184-1191; c) T. Schemme, E. Travkin, K. Ditte, W. Jiang, Z. Wang, C. Denz, *Opt. Mater. Express* **2012**, *2*, 856-863.

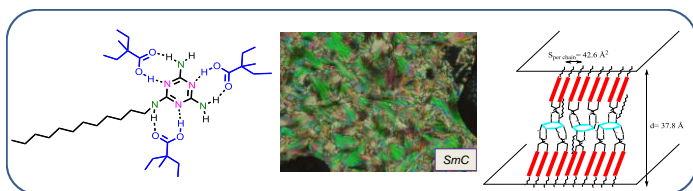
Received: ((will be filled in by the editorial staff))

Revised: ((will be filled in by the editorial staff))

Published online: ((will be filled in by the editorial staff))

## Entry for the Table of Contents

## FULL PAPER



Luminescence and photoconductivity properties of new supramolecular liquid crystalline dendrimers with an *s*-1,3,5-triazine core and fluorescent dendrons incorporated in the periphery are described.

## Liquid Crystals

*Madalina Bucos, Teresa Sierra, Attilio Golemme, Roberto Termine, Joaquín Barberá, Raquel Giménez, José Luis Serrano, Pilar Romero\* and Mercedes Marcos\*.*

■ ■ - ■ ■

**Multifunctional supramolecular dendrimers with an *s*-triazine ring as the central core. Liquid crystalline, fluorescence and photoconductive properties.**